SPECIAL REPORT 91-31

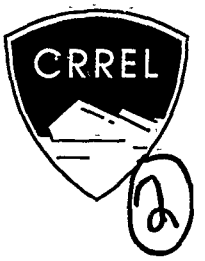

Creep and Yield Model of Ice under Combined Stress

Anatoly M. Fish

December 1991

For conversion of SI metric units to U.S./British customary units of measurement consult ASTM Standard E380, Metric Practice Guide, *published by the American Society for Testing and Materials, 1916 Race St., Philadelphia, Pa. 19103.*

This report is printed on paper that contains a minimum of 50% recycled material.

Special Report 91-31

U.S. Army Corps of Engineers
Cold Regions Research & Engineering Laboratory

Creep and Yield Model of Ice under Combined Stress

Anatoly M. Fish

December 1991

Prepared for
OFFICE OF THE CHIEF OF ENGINEERS

PREFACE

This report was prepared by Dr. Anatoly M. Fish, Research Civil Engineer, Civil and Geotechnical Engineering Research Branch, Experimental Engineering Division, U.S. Army Cold Regions Research and Engineering Laboratory. The work was funded under DA Project 4A762784AT42, *Design, Construction and Operations Technology for Cold Regions*, Task BS, Work Unit 013, *Improve Design Criteria for Foundations in Cold Regions.*

The author thanks Austin Kovacs and Dr. Devinder Sodhi for technical review of this report and valuable comments.

This report is dedicated to the memory of Dr. Andrew Assur.

CONTENTS

ILLUSTRATIONS

Creep and Yield Model of Ice under Combined Stress

ANATOLY M. FISH

INTRODUCTION

The successful solution of ice engineering problems depends greatly upon the accuracy of the constitutive laws and failure criteria of ice used in analyses of engineering structures. Two approaches can be distinguished in describing the deformation and failure processes of ice in uniaxial as well as multiaxial stress states.

In the first (traditional) approach, it is assumed that the total creep shear strain γ^c can be broken down into four components:

$$\gamma^c = \gamma_e + \gamma_p + \gamma_v + \gamma_t \tag{1}$$

where γ_e, γ_p, γ_v and γ_t are elastic, primary, secondary, and tertiary pure shear strain, respectively. In practice, however, to simplify the parameter evaluation procedure and/or to obtain closed-form solutions of boundary problems, some of the strain components in eq 1 are often ignored, and the time-dependent creep process in ice is portrayed by simplified models: primary ($\gamma_v = \gamma_t = 0$), secondary ($\gamma_p = \gamma_t = 0$), and tertiary ($\gamma_p = \gamma_v = 0$) creep equations, often represented by various mechanical models. Combined models such as attenuating ($\gamma_t = 0$), exponential ($\gamma_p = 0$), and other creep models are based explicitly or implicitly upon various combinations of the components of eq 1. The failure process, particularly time to failure, is either not considered (in most cases) or is assumed to take place in the later, secondary or tertiary stages of creep. Moreover, often the ice strength is considered a special field of study loosely related to the creep of ice.

In the second approach, deformation and failure of ice are considered to be a unified process that takes place in all stages of creep. Consequently, the creep process is not considered in terms of real time (t) but in terms of normalized time $\bar{t} = t/t_m$, where t_m is time to failure (Fish 1980, Morland and Spring 1981, and others).

Time to failure plays an extremely important role within the framework of this approach. It is one of the most important parameters that define the service lifetime of a structure. Time to failure unites all three stages of creep and failure, but it also combines creep and fracture, microcrack formation kinetics, recrystallization, and other processes that take place during deformation and failure of ice (Fish 1976).

The principal elements of the model, which was originlly developed (Fish 1976, 1980, 1983, 1987) to describe one-dimensional creep and failure of frozen soils and ice, and is expanded below for three-dimensional deformation, can also be approximately expressed in terms of the components of eq 1 as a product of primary, secondary, and tertiary creep strains, i.e.,

$$\gamma^c = \gamma_e + \gamma_p \gamma_m \gamma_t \tag{2}$$

where γ_m = Const. = viscous shear strain at failure. Both primary and tertiary creep strains are functions of normalized time, i.e., $\gamma_p = \gamma_p(\bar{t})$ and $\gamma_t = \gamma_t(\bar{t})$. Secondary creep is considered to be a point (M) on the creep curve (Fig. 1) defining time to failure. The stress dependency of the strain rate that reaches a minimum $(\dot{\gamma} = 0)$ at this point is described by a viscous flow equation which, as well as the time to failure function, includes a yield criterion of ice.

Thus the combined creep and yield model of ice under multiaxial stress developed in the following sections consists of four principal elements: a constitutive equation, a viscous flow equation and a yield criterion, all united by a time to failure function. One of the specific features of this model is that any of its elements can be replaced if it is found that other functions better represent the mechanical behavior of ice during creep.

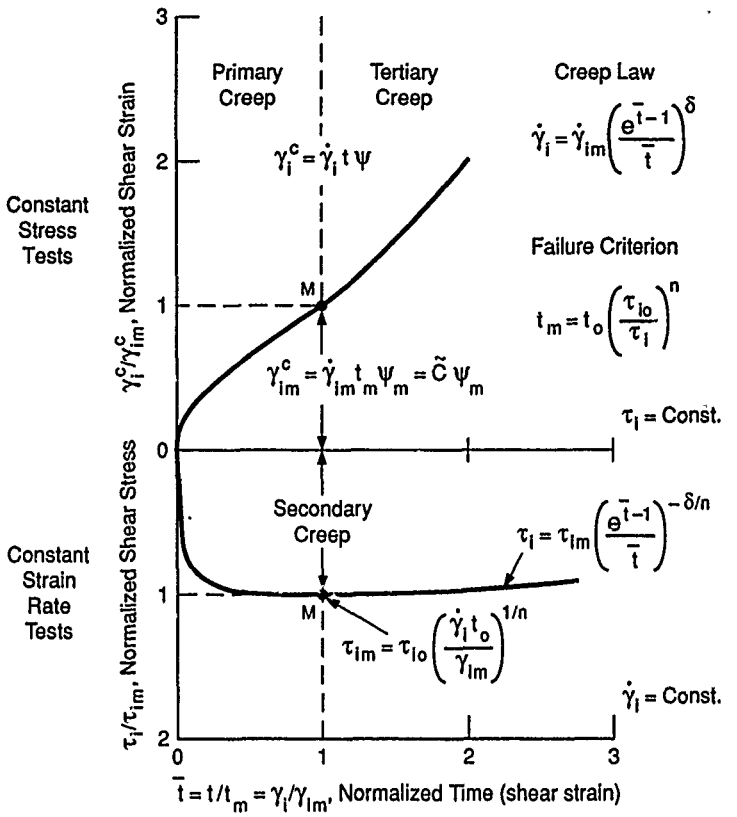

Figure 1. Creep model for ice in a multiaxial stress state (Fish 1983, 1984).

CREEP MODEL

Triaxial creep tests (τ_i = Const)

Constitutive equation

The entire deformation process, which includes primary, secondary, and tertiary short-term creep of homogeneous and isotropic ice under multiaxial stress at constant temperature, can be presented as a product of the flow equation and the nondimensional time function (Fish 1980, 1983):

$$\dot{\gamma}_i(\bar{t}) = \dot{\gamma}_{im} F(\bar{t}) \tag{3}$$

where $\dot{\gamma}_i(\bar{t}) = 2J_{2e}^{1/2}$ = shear strain rate (intensity)

$\dot{\gamma}_{im}$ = minimum shear strain rate

$J_{2e} = \frac{1}{6}\left[(\dot{\varepsilon}_1 - \dot{\varepsilon}_2)^2 + (\dot{\varepsilon}_2 - \dot{\varepsilon}_3)^2 + (\dot{\varepsilon}_3 - \dot{\varepsilon}_1)^2\right]$ = second invariant of the deviatoric strain rate tensor.

The nondimensional time function

$$F(\bar{t}) = \left(\frac{e^{\bar{t}-1}}{\bar{t}}\right)^{\delta} = \exp\left\{\delta\left(\bar{t} - \ln \bar{t} - 1\right)\right\} \tag{4}$$

where δ is the first shape parameter of a creep curve. Function $F(\bar{t})$ is such that for primary and tertiary creep $F(\bar{t}) > 1$, and for secondary creep (points M in Fig. 1) $t = t_m$, $\bar{t} = 1$, and $F(\bar{t}) = 1$. For ice, the value of δ is between 0.3 and 0.7 and has an average value of ~0.5 (Fish 1987).

Flow equation

The minimum shear strain rate is related to the time to failure by means of the flow equation

$$\dot{\gamma}_{im} = \frac{\tilde{C}}{t_m} \quad \text{or} \quad \dot{\gamma}_{im} t_m = \tilde{C} \tag{5}$$

where $\tilde{C}$ = the second shape parameter, which is equal to the viscous strain at failure. For polycrystalline ice $\tilde{C}$ is between 10^{-1} and 10^{-3}. Both δ and $\tilde{C}$ are assumed to be constant for a given ice temperature. The tilde (~) indicates that in the general case C may be a function of stress, temperature and other factors (Fish 1987, 1989).

Time to failure

When time $t = t_m$ the strain rate reaches a minimum $\dot{\gamma}_i = \dot{\gamma}_{im}$ $(\dot{\gamma}_i = 0)$, and it is assumed that failure occurs. In the framework of this model, time to failure t_m performs a crucial role: it not only unites all stages of creep, which makes it possible to describe the entire creep process under both constant stresses and constant strain rates by means of a single constitutive equation, but it also combines the long-term strength and the yield criteria of ice so that the latter can be incorporated into the constitutive equation of ice. The magnitude of shear stress that causes failure at time t_m can be expressed (Fish 1991) as a product of two independent functions: the yield function (criterion) and the nondimensional time function $\Phi(\tilde{t})$:

$$J_2 = J_{2o}\, \Phi^2(\tilde{t}) \tag{6}$$

where $J_{2o} = J_{2o}(I_1)$ is an "instantaneous" yield criterion, I_1 is the first invariant of the stress tensor, and J_2 is the second invariant of deviatoric stress tensor. By selecting the time function in the simplest form,

$$\Phi(\tilde{t}) = (t_m/t_o)^{-1/n}; \quad 1 \geq \Phi(\tilde{t}) \tag{7}$$

where $\tilde{t} = t_m/t_o$ = nondimensional time to failure
t_o = relaxation time (see eq 12 below)
n = parameter.

Combining eq 6 and 7, the failure or the long-term strength criterion of ice takes the form

$$t_m = t_o \left(\frac{J_{2o}}{J_2}\right)^{n/2} \tag{8}$$

or

$$t_m = t_o \left(\frac{\tau_{io}}{\tau_i}\right)^{n} \tag{9}$$

where $\tau_i = J_2^{1/2}$ and $\tau_{io} = J_{2o}^{1/2}$ can be defined as the shear stress and the "instantaneous" shear stress intensity (resultant) respectively (see eq 38 below).

Modified flow equation

Combining eq 5, 8 and 9, the flow equation of ice in a multiaxial stress state becomes

$$\dot{\gamma}_{im} = \frac{\tilde{C}}{t_o}\left(\frac{J_2}{J_{2o}}\right)^{n/2} = \frac{\tilde{C}}{t_o}\left(\frac{\tau_i}{\tau_{io}}\right)^{n} \tag{10}$$

or

$$\dot{\gamma}_{im} = \tilde{C}\,\frac{kT}{h}\, e^{-E/RT}\left(\frac{\tau_i}{\tau_{io}}\right)^{n} \tag{11}$$

where

$$t_o = \frac{h}{kT}\exp\left(\frac{E}{RT}\right) \tag{12}$$

and t_o = Frenkel's relaxation time (Frenkel 1947)
h = Planck's constant
k = Boltzmann's constant
T = absolute temperature
E = activation energy
R = gas constant.

Note that the flow equations (eq 10 and 11) are fundamentally different from the Norton-Glen (1958) flow law (see eq 43 below) although it contains a power function of stress. Parameters $\tilde{C}$ and t_o in eq 10 and 11 have a definite physical meaning, and the denominator of the stress function is a temperature-dependent yield criterion of ice (see eq 38 below). This yield criterion, which is a function of the first invariant of the stress tensor, relates the minimum shear strain rate and the shear stress in the whole spectrum of hydrostatic pressures (mean normal stresses). At the mean stress $\sigma_m < \sigma_{max}$ the first invariant serves as a depressant for the strain rate; i.e. the increase of the hydrostatic stress is accompanied by a decrease of the strain rate. When stress $\sigma_m > \sigma_{max}$ the increase of the hydrostatic stress enhances the creep rate that is confirmed by test data (Jones and Chen 1983).

The original Norton equation is more suitable for frictionless materials, such as metals, the creep behavior of which is unaffected by the first invariant of the stress tensor. If the combination of applied stresses is such that $\tau_i = \tau_{io}$ and $t_m = t_o$ then eq 10 becomes

$$\dot{\gamma}_{io} = \frac{\tilde{C}}{t_o} \tag{13}$$

where $\dot{\gamma}_{io} = \dot{\gamma}_{im}$ can be defined as the "instantaneous" shear strain rate, i.e., the rate at which the transition from the brittle to the ductile mode of failure takes place.

Creep shear strain

At constant stresses creep shear strains are obtained by integrating eq 3. The entire creep process as described by (Fish 1983) is

$$\gamma_i^c(t) = \frac{\tau_i}{G} + \dot{\gamma}_i\, t\, \psi \tag{14}$$

where τ_i = shear stress
G = shear modulus
$\gamma_i^c = 2J_{2e}^{1/2}$ = creep shear strain
$J_{2e} = \frac{1}{6}\left[(\varepsilon_1 - \varepsilon_2)^2 + (\varepsilon_2 - \varepsilon_3)^2 + (\varepsilon_3 - \varepsilon_1)^2\right]$ = second invariant of the deviatoric strain tensor
$\psi = \psi(\bar{t})$ = integration coefficient calculated depending upon the normalized time $\bar{t}$.

In the practical sense, the instantaneous strains are small and in many instances can be ignored, which substantially simplifies the parameter evaluation procedure. When $t = t_m$, $\bar{t} = 1$, and $\dot{\gamma}_i = \dot{\gamma}_{im}$, eq 14 gives an expression for failure shear strain (Fig. 1)

$$\gamma_{im}^c = \frac{\tau_i}{G} + \dot{\gamma}_{im} t_m \psi_m \tag{15}$$

where ψ_m is an integration coefficient calculated for $\bar{t} = 1$. The first term in the right side of eq 15 is the instantaneous strain and is ignored in the plot shown in Figure 1.

Combining eq 5 and 15

$$\gamma_{im}^c = \frac{\tau_i}{G} + \tilde{C}\psi_m = \frac{\tau_i}{G} + \frac{\tilde{C}}{\sqrt{\lambda}} \tag{16}$$

where $\psi_m \approx 1/(1-\delta)^{1/2} = \bar{\lambda}^{1/2}$ and $\lambda = 1 - \delta$. It is more convenient for the analysis of test data to use an approximate integral of eq 3 (Fish 1983, eq 38; Fish 1987, eq 20):

$$\gamma_i^c(\bar{t}) \approx \frac{\tau_i}{G} + \frac{\tilde{C}}{\sqrt{\lambda}}\,\bar{t}^{\lambda} e^{\delta_1(\bar{t}-1)} \tag{17}$$

where $\delta_1 = \lambda^{1/2} - \lambda$. Defining $\tilde{C}(t) = \dot{\gamma}_{im} t$ and combining eq 5 and 17 the entire creep process can be expressed in terms of viscous (nonrecoverable) shear strain only:

$$\gamma_i^c(\bar{t}) \approx \frac{\tau_i}{G} + \frac{\tilde{C}}{\sqrt{\lambda}}\left(\frac{\tilde{C}(t)}{\tilde{C}}\right)^{\lambda} e^{\delta_2[\tilde{C}(t) - \tilde{C}]} \tag{18}$$

where $\delta_2 = \delta_1/\tilde{C}$.

Thus, the entire creep process in ice in a multiaxial stress state at constant stresses is described by means of only two parameters, $\tilde{C}$ and $\delta(\lambda)$, to be determined from test data. An evaluation procedure for these parameters is presented in Fish (1983, 1987, 1989).

Triaxial constant strain rate tests ($\dot{\gamma}_i$ = Const.)

Strength criterion

If the tests are carried out in such a manner that the shear strain rate is maintained constant (strength tests) at $\dot{\gamma}_i = \dot{\gamma}_{im}$, the shear stress becomes a function of this rate. Defining $\gamma_i = \dot{\gamma}_i t$, $\gamma_{im} = \dot{\gamma}_{im} t_m$, and $\tilde{C} = \gamma_{im}$, and combining the latter with eq 10,

$$\tau_{im} = \tau_{io}\left(\frac{\dot{\gamma}_i t_o}{\gamma_{im}}\right)^{1/n}. \tag{19}$$

where τ_{io} is a yield criterion (eq 38 below). Subscript m indicates that the magnitudes of stress (τ_{im}) and strain (γ_{im}) are referred to the point M corresponding to the maximum (peak) shear stress in Figure 1.

If $\dot{\gamma}_i = \dot{\gamma}_{io}$ then $\gamma_{im} = \gamma_{io} = \dot{\gamma}_{io} t_o$ and $\tau_{im} = \tau_{io}$, and eq 19 will coincide with eq 13; i.e., the maximum (peak) shear stress will coincide with the yield stress.

Stress–strain relationship

Stress-strain relationships outside point M (Fig. 1) are obtained by combining and rearranging eq 3, 4, and 19:

$$\tau_i = \tau_{im}\left(\frac{e^{\bar{t}-1}}{\bar{t}}\right)^{-\delta/n} \tag{20}$$

or

$$\tau_i = \tau_{im}\left(\frac{\gamma_i}{\gamma_{im}}\right)^{\delta/n} \exp\left[-\frac{\delta}{n}\left(\frac{\gamma_i}{\gamma_{im}} - 1\right)\right] \tag{21}$$

where $\bar{t} = t/t_m = \gamma_i/\gamma_{im} = \bar{\gamma}$, and $\tau_i = \tau_i(\bar{t}) = \tau_i(\bar{\gamma})$. For secondary creep, $\bar{t} = 1$ and the strain rate dependency of stress is defined by eq 19.

YIELD MODEL

Extended von Mises criterion

Analysis of test data shows that at low stress levels (Haynes 1975) or low strain rates (Hawkes and Mellor 1972) the strength of ice is independent of confining pressure, the angle of internal friction of ice approaches zero, and ice may be considered as an ideally cohesive material whose yield criterion may be selected in the form of either the von Mises or the Tresca rupture models. On the other hand, triaxial tests carried out at relatively

high stresses, high strain rates and/or high confining pressures (Sayles 1974, Jones 1978, 1982, Hausler 1982, Richter-Menge et al. 1986 and others) indicate that the strength of ice is a nonlinear function of the confining pressure. Sayles (1974) showed that the angle of internal friction of ice differs from zero. Moreover, at a certain level of confining pressure the strength of ice reaches a maximum value (Jones 1978) associated with the ice melting pressure. The yield function of such a material can be expressed in terms of the extended von Mises or Mohr-Coulomb rupture models (Fish 1991), and in the former case by expanding the von Mises criterion into the series

$$J_2^{1/2} = d + d_1 I_1 + d_2 I_1^2 + d_3 I_1^3 + d_4 I_1^4 \ldots \tag{22}$$

where J_2 = second invariant of the deviatoric stress tensor
I_1 = first invariant of the stress tensor
$d, d_{1,2,3,4}$ = parameters.

By retaining only the first term on the right side of eq 22 it becomes von Mises' yield criterion; the first two terms—the von Mises-Drucker-Prager criterion; three terms—Nadai's type yield criterion (Nadai 1950; Smith 1974; and others); four terms—the teardrop model for ice (Nadreau and Michel 1986, 1986a); etc. We will limit ourselves to consideration of the second-order polynomial function as the simplest nonlinear yield function whose parameters can be easily determined from test data.

Parabolic yield criterion

Let us assume that the compressive stresses are positive. Then the strength of ice in a multiaxial stress state can be described by a parabolic yield criterion in Figure 2 (Fish 1991):

$$\tau_i = c + b\sigma_m - \frac{b}{2\sigma_{max}}\sigma_m^2 \tag{23}$$

where

$$\tau_i = J_2^{1/2} = \frac{1}{\sqrt{6}}\left[(\sigma_1-\sigma_2)^2 + (\sigma_2-\sigma_3)^2 + (\sigma_3-\sigma_1)^2\right]^{1/2}$$

is shear stress (intensity) and

$$\sigma_m = \frac{I_1}{3} = \frac{1}{3}(\sigma_1 + \sigma_2 + \sigma_3) = \text{mean normal stress}$$

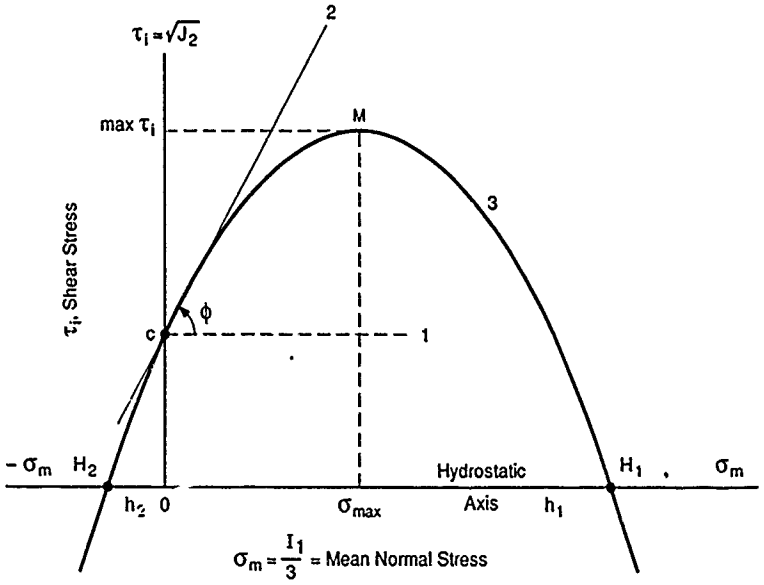

$$\tau_i = c + b\sigma_m - \frac{b}{2\sigma_{max}}\sigma_m^2$$

$$\max \tau_i = c + \frac{b}{2}\sigma_{max}$$

$$h_{1,2} = \sigma_{max} \pm \left[\sigma_{max}^2 + \frac{2c}{b}\sigma_{max}\right]^{\frac{1}{2}}$$

$$b = \tan\phi$$

Figure 2. Yield criteria of ice: 1–von Mises, 2–Drucker-Prager, 3–Parabolic (Fish 1991).

$\sigma_1, \sigma_2, \sigma_3$ = principal stresses

c = resistance in pure shear associated with the ice cohesion on the octahedral plane

$b = \tan\phi$ and ϕ = angle of internal friction on the octahedral plane

σ_{max} = ice melting pressure, i.e., the magnitude of the mean normal stress at which the shear stress of ice reaches a maximum:

$$\max \tau_i = c + \frac{b}{2}\sigma_{max}. \tag{24}$$

The yield curve intersects the hydrostatic axis at points $H_{1,2}$, the abscissas of which are

$$h_{1,2} = \sigma_{max} \pm \left[\sigma_{max}^2 + \frac{2c}{b}\sigma_{max}\right]^{1/2}. \tag{25}$$

Note that the yield curve shape is defined by the ratio of parameters c and b.

Equation 23 can be considered as an extended von Mises-Drucker-Prager yield criterion. At low stress levels ($\sigma_{max} \to \infty$), eq 23 transforms into the Drucker-Prager (1952) yield criterion. For frictionless materials ($b = 0$), eq 23 reduces to the von Mises yield criterion. Parameter σ_{max} may be regarded as one of the fundamental physical characteristics of ice, probably closely related to the phase changing pressure (point H_1) for a given temperature (Nadreau and Michel 1986; Hallam and Nadreau 1988). Point H_2 with abscissa h_2 may be considered as the resistance of ice to triaxial extension. Introduction of a new ice physical characteristic σ_{max} and ratio $b/2\sigma_{max}$ in eq 23 makes the latter different from the known parabolic yield criteria of Nadai (1950), Smith (1974), and others. Instead of the ratio $b/2\sigma_{max}$ these authors use the parameter d_2 (eq 22), the physical meaning of which is uncertain and the magnitude of which will be dependent of the strain rate (or time to failure). Therefore, these criteria cannot be applied to describe the test data plotted below with a single set of the strength parameters.

Thus ice strength in a multiaxial stress state can be described by a yield criterion (eq 23), three parameters of which—c, $b(\phi)$ and σ_{max}—have a definite physical meaning and can be determined from test data.

LONG-TERM STRENGTH

Triaxial creep tests (τ_i = Const.)

It has been mentioned above that the creep strength of ice is a function of time or the applied strain rate. The absolute values of ice strength as well as the magnitudes of the strength parameters change from the greatest (instantaneous) values at the time of loading (t_o) to zero for longer time intervals. Consequently the creep strength of ice will not be characterized by a single yield curve but by a family of curves for given times $t_o < t_1 < t_n$ (Fig. 3) or given strain rates $\dot{\gamma}_{io} > \dot{\gamma}_{i1} > \dot{\gamma}_{in}$. During creep at constant stress, the strength parameters in eq 23, except σ_{max}, become functions of time to failure:

$$\tau_i(t) = c(t) + b(t)\sigma_m - \frac{b(t)}{2\sigma_{max}}\sigma_m^2 \tag{26}$$

where $c(t)$ and $b(t) = \tan\phi(t)$ are the cohesion and this friction angle, on the octahedral plane, at time $t = t_m$, respectively. The ice strength reaches its maximum when

$$\max \tau_i(t) = c(t) + \frac{b(t)}{2}\sigma_{max}. \tag{27}$$

Note that the shape of the creep strength curves and the abscissas of points H_1 and H_2 in Figure 3 are dependent upon the ratio of parameters $c(t)$ and $b(t)$ and their change with time:

$$h_{1,2}(t) = \sigma_{max} \pm \left[\sigma_{max}^2 + \frac{2c(t)}{b(t)}\sigma_{max}\right]^{1/2}. \tag{28}$$

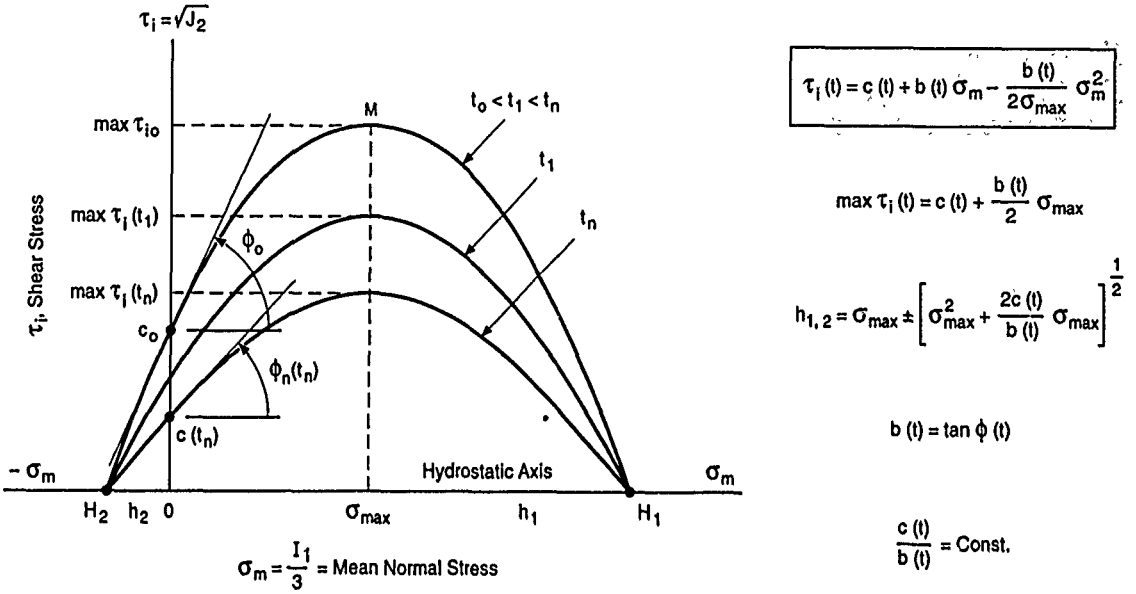

Figure 3. Creep strength criterion (Fish 1991).

As a first approximation one may assume that this ratio

$$\frac{c(t)}{b(t)} = \text{Const} \tag{29}$$

i.e., the coordinates of the points $H_{1,2}$ during creep, remain unchanged and all the curves will have common intercepts. At low stress levels or when $\sigma_{max} \to \infty$, eq 26 reduces to the von Mises-Drucker-Prager strength criterion expanded for creep conditions:

$$\tau_i(t) = c(t) + b(t)\sigma_m \tag{30}$$

and when $b = 0$ it reduces to the von Mises strength criterion

$$\tau_i(t) = c(t)\,, \tag{31}$$

in which parameters c and b are functions of time.

Triaxial constant strain rate tests ($\dot{\gamma}_i$ = Const .)

For constant strain rate (strength) tests $t_m = \gamma_i/\dot{\gamma}_i = \gamma_{im}/\dot{\gamma}_{im}$, $t_o = \gamma_{io}/\dot{\gamma}_{io}$. Then the parameters of eq 26 through 31 as well as the strength criteria of ice become functions of the shear strain rate (and strain), i.e.:

$$\tau_i(\dot{\gamma}_i) = c(\dot{\gamma}_i) + b(\dot{\gamma}_i)\sigma_m - \frac{b(\dot{\gamma}_i)}{2\sigma_{max}}\sigma_m^2 \tag{32}$$

$$\max\tau_i(\dot{\gamma}_i) = c(\dot{\gamma}_i) + \frac{b(\dot{\gamma}_i)}{2}\sigma_{max} \tag{33}$$

and

$$h_{1,2}(\dot{\gamma}_i) = \sigma_{max} \pm \left[\sigma_{max}^2 + \frac{2c(\dot{\gamma}_i)}{b(\dot{\gamma}_i)}\sigma_{max}\right]^{1/2}. \tag{34}$$

When $\sigma_{max} \to \infty$ and $b \neq 0$,

$$\tau_i(\dot{\gamma}_i) = c(\dot{\gamma}_i) + b(\dot{\gamma}_i)\sigma_{max}\,. \tag{35}$$

When $b = 0$,

$$\tau_i(\dot{\gamma}_i) = c(\dot{\gamma}_i). \tag{36}$$

For constant strain rate tests the creep strength criterion depicted in Figure 3 will retain its original meaning. However, the time functions of the strength parameters in it must be replaced by functions of shear strain rates (Fig. 4). The creep strength curves will have common intercepts—points $H_{1,2}$ if the ratio

$$\frac{c(\dot{\gamma}_i)}{b(\dot{\gamma}_i)} = \text{Const.} \tag{37}$$

If this ratio varies, i.e., if the rates of change of parameters c and b are different, the curves will intersect.

Time-dependent failure

Passing vertical planes through point M in Figure 3 one obtains the relationship between the creep strength of ice τ_i and the time to failure t_m. Such a dependency relates the (instantaneous) yield function of ice determined from creep tests at time t_o (or from constant strain rate tests at the shear strain rate $\dot{\gamma}_{io}$) with a creep strength $\tau_i(t) = \tau_i(t_m)$ determined at times $t_m = t_1, \ldots t_n$ etc.

It has been shown elsewhere (Fish 1991) that the creep strength criterion (eq 26) can be expressed as a product of the yield function (eq 23) and the nondimensional time function (eq 7), i.e.

$$\tau_i = \tau_{io}\Phi(\tilde{t}) \tag{6}$$

when $t_m = t_o$, $\Phi(\tilde{t}) = 1$ and

$$\tau_{io} = c + b_o\sigma_m - a_o\sigma_m^2 \tag{38}$$

$$a_o = b_o/2\sigma_{max}, \quad b_o = \tan\phi_o.$$

Subscript 0 indicates that the failure shear stress or the strength parameters are referred to the instantaneous yield conditions. Comparing eq 6, 7, 9, 26, and 38

$$\Phi(\tilde{t}) = \frac{\tau_i(t)}{\tau_{io}} = \frac{b(t)}{b_o} = \frac{c(t)}{c_o} = (t_m/t_o)^{-1/n}. \tag{39}$$

Consequently, for constant strain rate tests ($\tau_i = \tau_{im}$) eq 39 takes the form

$$\Phi(\tilde{t}) = \Phi(\dot{\gamma}_i) = \frac{\tau_i(\dot{\gamma}_i)}{\tau_{io}} = \frac{b(\dot{\gamma}_i)}{b_o} = \frac{c(\dot{\gamma}_i)}{b_o} = \left(\frac{\gamma_{im}}{\dot{\gamma}_i t_o}\right)^{-1/n}. \tag{40}$$

Note that the two parameters t_o and n define the shapes of the curves of the long-term strength of ice. Analysis of Jones' data (Nadreau and Michel 1986a) showed that for ice under triaxial compression the exponent n changes insignificantly. However, the magnitude of n increases slightly when the confining pressure is zero. It has been shown (Fish 1991) for frozen soils at six different types of loading (uniaxial compression and tension, pure shear, and triaxial compression at three different mean normal stresses) that, for practical purposes, these parameters may be considered to be independent of the loading regime.

Thus the entire process of deformation and failure of ice in a multiaxial stress state at both constant stresses and constant strain rates is described by seven parameters:

Creep $\delta(\lambda)$ and $\tilde{C}$

Failure time t_o and n

Yield c_o, $b_o(\phi_o)$, and σ_{max}

which are determined from test data.

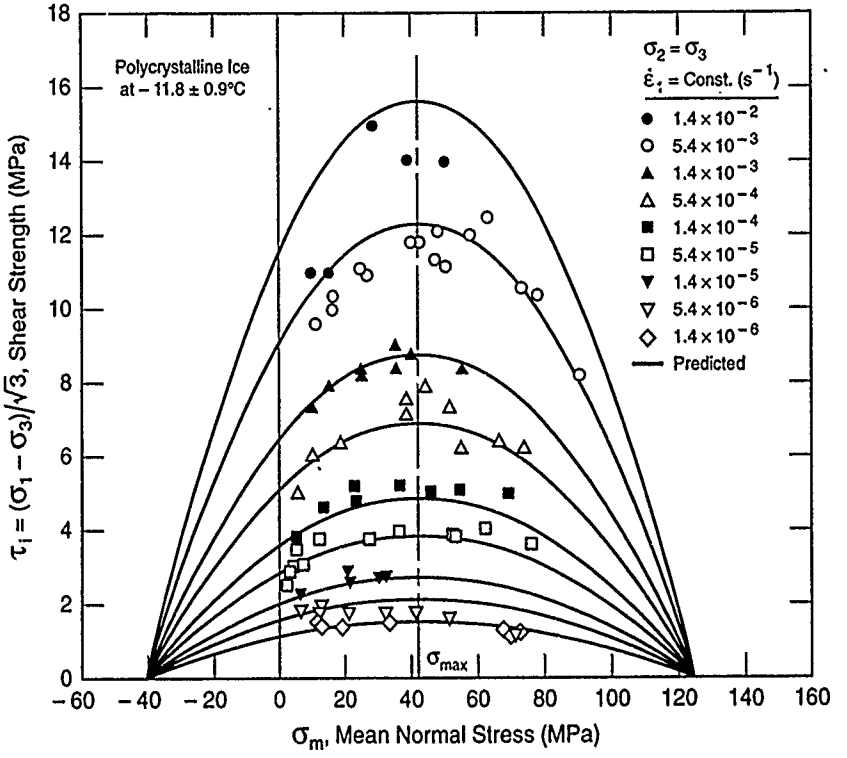

Figure 4. Strength of polycrystalline ice under triaxial compression ($\sigma_1 > \sigma_2 = \sigma_3$) at –11.8°C (data from Jones, 1982).

TEST DATA

Yield of ice under triaxial compression

The triaxial constant strain rate tests used in the present analysis were performed by Jones (1982). The freshwater ice used in them had a randomly oriented polycrystalline structure. The laboratory-made ice samples were 20 mm in diameter and 60 mm long. The axial strain rate $\dot{\varepsilon}_1$ varied between 10^{-7} and 10^{-1} s^{-1} and the confining pressure ($\sigma_2 = \sigma_3$) ranged from 0.1 to 85 MPa. The tests were carried out at –11.8° ±0.9°C. The test data were recalculated by this author in terms of the shear stress (τ_i) versus the mean normal stress, σ_m, and are presented in Figure 4.

Strictly speaking, this type of triaxial test can only approximately be considered as a pure constant strain rate regime. Indeed, during each test the axial strain was applied at a certain rate (constant strain rate regime), while the confining pressure which corresponds to a creep regime at constant stress was maintained constant.

Nevertheless, as a first approximation one may assume that eq 19 can be applied to this type of test. For tests when $\sigma_1 > \sigma_2 = \sigma_3$ it takes the form

$$\tau_{im} = \tau_{io} \left(\frac{(\dot{\varepsilon}_1 + \dot{\varepsilon}_3) t_o}{(\varepsilon_1 + \varepsilon_3)_{im}} \right)^{1/n} . \tag{41}$$

Unfortunately, values of $\dot{\varepsilon}_3$, ε_1, ε_3 and t_o are unavailable; therefore eq 41 is approximated by

$$\tau_{im} = \tau_{io} \left(\frac{\dot{\varepsilon}_1}{\dot{\varepsilon}_{10}} \right)^{1/n} \tag{42}$$

where $\dot{\varepsilon}_{10} = (\varepsilon_1 - \varepsilon_3)/t_o$ can be defined as the "instantaneous" strain rate. Such an approximation will not affect considerably the final calculations of the ice strength. Note that eq 42 is a simplified version of eq 19. For the analysis of the test data in Figure 4. Jones (1982) used Norton-Glen's power function

$$\dot{\varepsilon}_1 = A \, (\sigma_1 - \sigma_3)^n . \tag{43}$$

Jones also found that exponent $n = 3.95$, and that at strain rates $\dot{\varepsilon}_1 \approx 5.4 \times 10^{-2}\ s^{-1}$ and above the ice strength practically does not change. Therefore, for this particular type of ice and for the given test temperature this rate can be considered an "instantaneous" strain rate. Since eq 42 and 43 have the same (power) structure the exponent n can be used in the following analysis.

Then the magnitudes of the instantaneous shear stress as a function of the mean stress $\tau_{io} = f(\sigma_m)$ can easily be calculated by eq 42 using test data from Figure 4. After that the parameters of the yield criterion can be calculated by eq 38 and 25.

Based upon a regression analysis of all 86 tests the parameters of the yield criterion turned out to be

$c_o = 16.4$ MPa
$b_o = 0.27$
$\phi_o \approx 15°$
$\sigma_{max} = 41.5$ MPa
$h_1 = 123.7$ MPa
$h_2 = -40.7$ MPa .

Both the experimental and predicted (by eq 38, 40 and 42) values of the ice shear strength under triaxial compression at various axial strain rates and at various mean normal stresses are presented in Figure 4. One can conclude that equations developed fit the test data quite well.

It is interesting to note that the magnitude of σ_{max} (41.5 MPa) is in agreement with that found by Jones (~40 MPa). The magnitude of the intersect ($h_1 = 123.7$ MPa) is in agreement with the value (~120 MPa) suggested in Hallam and Nadreau (1988).

Note that the instantaneous value of the ice friction angle turned out to be very small ($\phi_o \approx 15°$). Both the friction angle and the cohesion decrease rapidly with decreasing strain rate, and at a strain rate of $\sim 10^{-6}\ s^{-1}$ the friction angle magnitude $\phi \approx 1°$. That means that the ice gradually transforms from a material that at high strain rates possesses both the cohesion and the friction angle into an ideally cohesive material the shear strength of which may be described by a the von Mises (eq 36) or the Tresca strength criterian expanded for creep conditions. The latter is a particular case of a more general parabolic (extended) Mohr-Coulomb strength criterion that also can be applied to describe the entire family of yield surfaces in Figure 4 (Fish 1991).

Creep of ice under triaxial compression

Triaxial tests of ice used in the creep analysis were performed by Golubov et al. (1990) using laboratory-made samples of saline ice. The test samples were 45.1 mm in diameter and 100 mm long. The diameter of the randomly oriented ice crystals varied between 0.5 and 1.5 mm. The density of the ice was 0.85 to 0.9 g/cm^3 and average salinity was ~5‰. The tests were carried out at -5°C ±0.2°C.

Prior to the creep tests a series of strength tests were conducted at a constant strain rate and various confining pressures ($\sigma_2 = \sigma_3$). The data from these tests were recalculated in terms of $\tau_i = f(\sigma_m)$ and are presented in Figure 5. The strain rate at which the tests were conducted was not specified, but comparison with the creep tests shown in Figure 6 brings us to the conclusion that the strength test strain rate was higher than the secondary creep rate in the creep tests. Therefore, the data in Figure 5 can be used for determining the strength parameters of the saline ice. The tests were conducted under considerably smaller mean normal stresses than the tests of Jones (Fig. 4). Therefore the test data can be approximated by the linear von Mises-Drucker-Prager yield criterion (eq 38 at $a_o = 0$). The magnitudes of the strength parameters of the saline ice at - 5°C turned out to be

$$c_o = 0.58 \text{ MPa} \quad \text{and} \quad b_o = 0.11 \ (\phi_o \approx 6°)$$

which are considerably smaller than those of freshwater polycrystalline ice at -11.8°C.

The results of the triaxial creep tests are presented in Figure 6. These tests were carried out at constant shear stress $\tau_i = (\sigma_1 - \sigma_3)/\sqrt{3} = 0.46$ MPa and at three different magnitudes of the mean normal stress ($\sigma_m = 1.18$, 2.18 and 4.18 MPa). From a cursory analysis of the test data one can conclude that when all other conditions are equal the creep shear strain and the strain rate in ice substantially depend upon the mean normal stress as predicted by eq 10.

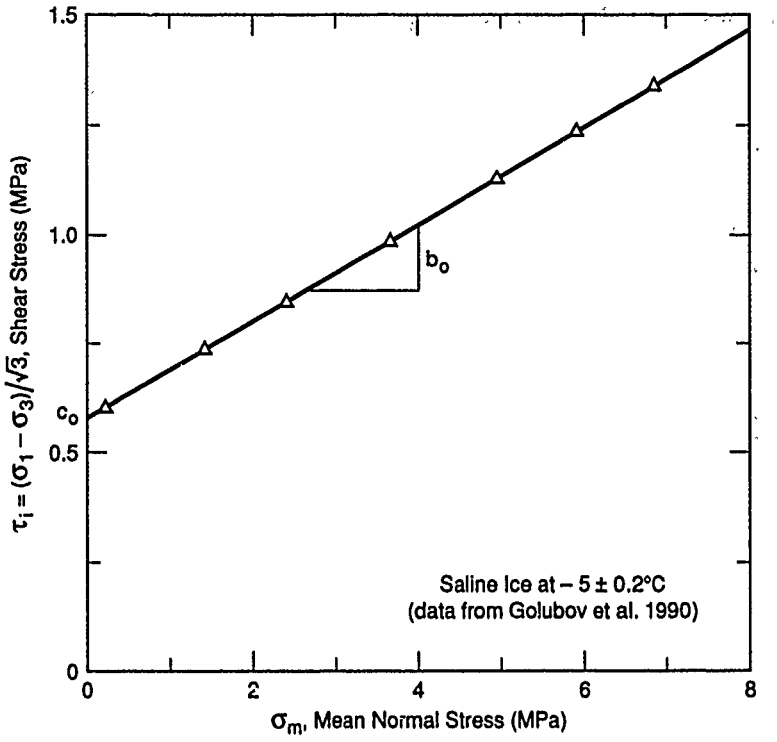

Figure 5. Strength of saline ice under triaxial compression ($\sigma_1 > \sigma_2 = \sigma_3$) at –5 °C (data from Golubov et al. 1990).

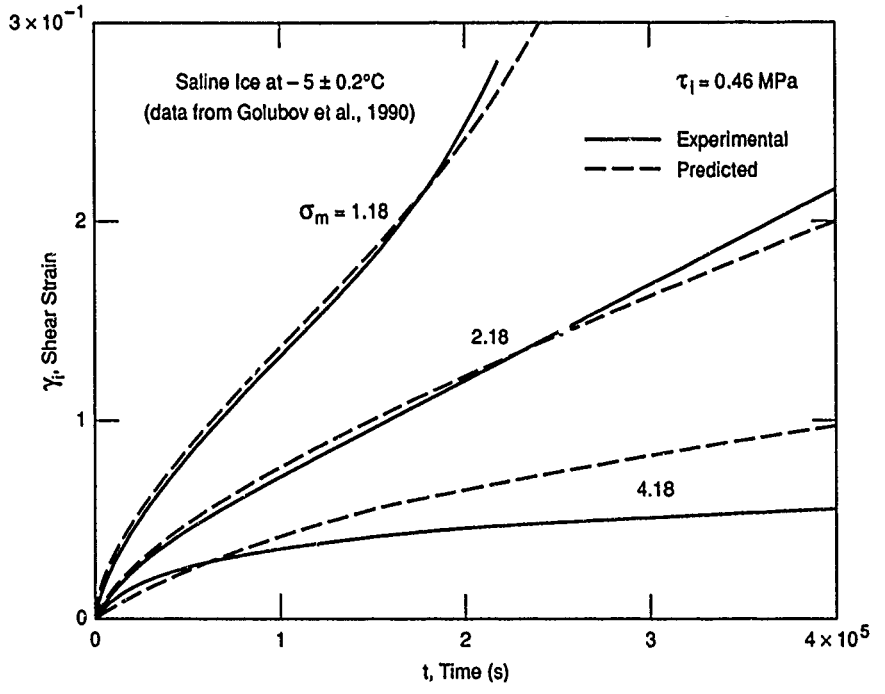

Figure 6. Creep of saline ice at –5 °C under triaxial compression ($\sigma_1 > \sigma_2 = \sigma_3$) at constant shear stress τ_i = 0.46 MPa and various mean normal stresses σ_m = 1.18; 2.18 and 4.18 MPa (data from Golubov et al. 1990).

The plot in Figure 6 contains both the experimental and predicted creep curves. The latter were calculated by eq 5, 9, 10, 17 and 38 using the following magnitudes of the creep parameters: $\tilde{C} = 0.1$; $\lambda = 0.57$; $\delta_1 = 0.185$; $n = 5.46$; $t_o = 6.63 \times 10^3$ s; and c_o and b_o obtained from the test data, assuming that the instantaneous strains are small and can be ignored. One can conclude that correspondence between the experimental and predicted creep shear strains is quite good, taking into account the fact that a single set of parameters was used in the calculations, together with a very limited amount of test data.

CONCLUSIONS

1. A combined creep and yield model has been developed for ice under multiaxial stresses for both constant stress and constant strain rate loading regimes. The creep model (Fish 1980, 1983) describes the entire (primary, secondary and tertiary) creep process in ice in terms of shear strain and consists of four principal elements: a constitutive equation, a flow (secondary creep) equation and a yield criterion, all united by a time to failure function.

2. Secondary creep is considered to be a transition point from primary to a tertiary creep stages defining time to failure. The strain rate at this point is a function of both the second invariant of the deviatoric stress tensor (J_2) (shear stress) and the first invariant of the stress tensor (I_1) (hydrostatic pressure). The stress dependency of the secondary (minimum) creep strain rate at failure is described by a modified Norton-Glen (power) equation, which as well as the time to failure function, include a yield criterion for ice.

3. The yield model is selected in the form of the (parabolic) extended von Mises-Drucker-Prager or the extended Mohr-Coulomb yield criterion (Fish 1991) in which the ice strength is characterized by three parameters: the cohesion c and the friction angle ϕ, on the octahedral plane, and the ice melting pressure σ_{max}, i.e. the magnitude of the mean normal stress at which the shear strength of ice reaches a maximum value.

4. The model has been verified using test data on the strength of freshwater polycrystalline ice at –11.8°C (Jones 1982) and creep of saline ice at –5°C (Golubov et al. 1990), both under triaxial compression.

SELECTED BIBLIOGRAPHY

Alkire, B.D. and O.B. Andersland (1973) The effect of confining pressure on mechanical properties of sand–ice materials. *Journal of Glaciology*, **13** (66): 469–481.

Ashby, M.F. and P. Duval (1985) The creep of poycrystalline ice. *Cold Regions Science and Technology*, **11**: 285–300.

Budd, W.F. and T.H. Jacka (1989) A review of the ice rheology for ice sheet modeling. *Cold Regions Science and Technology*, **16**: 107–144.

Colbeck, S.C. and R.J. Evans (1973) A flow law for temperate glacier ice. *Journal of Glaciolology*, **12**: 71–86.

Drucker, D.C. and W. Prager (1952) Soil mechanics and plastic analysis of limit design. *Quarterly Journal of Applied Mathematics*, **10**: 157–165.

Fish, A.M. (1976) An acoustic and pressure meter method for investigation of the rheological properties of ice. Ph.D. thesis, Arctic and Antarctic Research Institute, Leningrad, U.S.S.R. (translated from Russian, 1978). (Also USA Cold Regions Research and Engineering Laboratory, Internal Report 846 [unpublished]).

Fish, A.M. (1980) Kinetic nature of the long-term strength of frozen soils. In *Proceedings, 2nd International Symposium on Ground Freezing, 24–26 June, Trondheim, Norway* (P.E. Frivik, Ed.). Norwegian Institute of Technology, p. 95–108.

Fish, A.M. (1983) Thermodynamic model of creep at constant stress and constant strain rate. USA Cold Regions Research and Engineering Laboratory, CRREL Report 83-33. (Also *Cold Regions Science and Technology*, 9(2): 143–161, 1984.)

Fish, A.M. (1987) Shape of creep curves in frozen soils and polycrystalline ice. *Canadian Geotechnical Journal*, 24: 623–629.

Fish, A.M. (1989) Some peculiarities of creep behavior of frozen silt. In *Proceedings of the 8th International Conference on Offshore Mechanics and Arctic Engineering, The Hague, The Netherlands*, vol. 1, p. 721–724.
Fish, A.M (1991) Strength of frozen soil under a combined stress state. In *Proceedings of the Sixth International Symposium on Ground Freezing. Beijing, China, 10–12 September 1991*, vol. 1, p. 135–145.
Frenkel, J.I. (1947) *Kinetic Theory of Liquids*. Oxford: Clarendon Press.
Glen, J.W. (1958) The flow law of ice. In Physics of the movement of the ice. In *Proceedings of the Chamonix Symposium, September*. IASH Publication no. 47, p. 171–183.
Golubov, A.I., Razbegin, V.N. and M.E. Slepak (1990) Creep of saline ice under multiaxial stresses. In *Problems of Soil Mechanics and Permafrost Engineering* (Yu.K. Zaretsky, Ed.). Moscow, Stroyizdat (in Russian).
Hallam, S. and J.P. Nadreau (1988) Failure maps for ice. In *Proceedings, 9th International Conference on Port and Ocean Engineering under Arctic Conditions (POAC '87), 17–22 August, Fairbanks, Alaska* (W.M. Sackinger and M.O. Jeffries, Eds.). Geophysical Institute, University of Alaska–Fairbanks, vol. 3, p. 45–55.
Hausler, F.U. (1982) Multiaxial compressive strength tests on saline ice with brush-type loading platens. In *Proceedings of IAHR Symposium on Ice, 27–31 July, Université Laval, Quebec City, Quebec*. International Association for Hydraulic Research, vol. 2, p. 526–539.
Hawkes, I. and M. Mellor (1972) Deformation and fracture of ice under uniaxial stress. *Journal of Glaciology*, **11**(61): 103–131.
Haynes, F.D. (1973) Tensile strength of ice under triaxial stresses. USA Cold Regions Research and Engineering Laboratory, Research Report 312.
Hill, R. (1950) *The Mathematical Theory of Plasticity*. Oxford: Clarendon Press.
Jones, S.J. (1978) Triaxial Testing of Polycrystalline Ice. In *Proceedings, 3rd International Conference on Permafrost, 10–13 July, Edmonton, Alberta*. Ottawa: National Research Council of Canada, vol. 1, p. 217–245.
Jones, S.J. (1982) The confined compressive strength of polycrystalline ice. *Journal of Glaciology*, **20**(98): 171–177.
Jones, S.J. and H.A.M. Chew (1983) Creep of ice as a function of hydrostatic pressure. *Journal of Physical Chemistry*, **87**(21): 4064–4066.
Mellor, M. and D.M. Cole (1983) Stress/strain/time relations for ice under uniaxial compression. *Cold Regions Science and Technology*, **6**: 207–230.
Michel, B. (1978) *Ice Mechonics*. Les Presses de L'Université Laval, Quebec City, Quebec, 298 pp.
Morland, K.W. and U. Spring (1981) Viscoelastic fluid relation for the deformation of ice. *Cold Regions Science and Technology*, 4: 255–268.
Nadai, A. (1950) *Theory of Flow and Fracture of Solids*. New York: McGraw-Hill, vol. 1.
Nadreau, J.P. and B. Michel (1986) Yield and failure envelope for ice under multiaxial compressive stresses. *Cold Regions Science and Technology*, **13**(1): p. 75–82.
Nadreau, J.P. and B. Michel (1986a) Secondary creep in confined ice samples. In *Proceedings of 8th IAHR Symposium on Ice, 18–22 August, Iowa City, Iowa*. International Association for Hydraulic Research, vol. 1, p. 307–318.
Nevel, D.E. (1976) Creep theory for a floating ice sheet. USA Cold Regions Research and Engineering Laboratory, Special Report 76-4.
Richter-Menge, J.A., G.F.N. Cox, N. Perron, G. Durell and H.W. Bosworth (1986) Triaxial testing of first-year sea ice. USA Cold Regions Research and Engineering Laboratory, CRREL Report 86-16.
Sayles, F.H. (1974) Triaxial constant strain rate tests and triaxial creep tests on frozen Ottawa sand. USA Cold Regions Research and Engineering Laboratory, Technical Report 253.
Shyam, S., Sunder and Mao S. Wu (1989) A differential flow model for polycrystalline ice. *Cold Regions Science and Technology*, **16**: 41–62.
Sinha, N.K. (1978) Rheology of columnar-grained ice. *Experimental Mechanics*, **18**: 464–470.
Smith, M.B. (1974) A parabolic yield condition for anisotropic rocks and soils. Ph.D. Thesis (unpublished), Rice University, Houston, Texas.
Wilshire, B. and D.R.J. Owen (1982) *Recent Advances in Creep and Fracture of Engineering Materials and Structures*. Swansea, U.K.: Pineridge Press.
Vialov, S.S. (1986) *Rheological Fundamentals of Soil Mechanics*. Amsterdam, The Netherlands: Elsevier Science Publishers, B.V.

*U.S. GOVERNMENT PRINTING OFFICE: 1992-600-063/42062

REPORT DOCUMENTATION PAGE

Form Approved
OMB No. 0704-0188

1. AGENCY USE ONLY (Leave blank)	2. REPORT DATE	3. REPORT TYPE AND DATES COVERED
	December 1991	

4. TITLE AND SUBTITLE

Creep and Yield Model of Ice under Combined Stress

5. FUNDING NUMBERS

PR: 4A762784AT42
TA: BS
WU: 013

6. AUTHORS

Anatoly M. Fish

7. PERFORMING ORGANIZATION NAME(S) AND ADDRESS(ES)

U.S. Army Cold Regions Research and Engineering Laboratory
72 Lyme Road
Hanover, New Hampshire 03755-1290

8. PERFORMING ORGANIZATION REPORT NUMBER

Special Report 91-31

9. SPONSORING/MONITORING AGENCY NAME(S) AND ADDRESS(ES)

Ofice of the Chief of Engineers
Washington, D.C. 20314-1000

10. SPONSORING/MONITORING AGENCY REPORT NUMBER

11. SUPPLEMENTARY NOTES

12a. DISTRIBUTION/AVAILABILITY STATEMENT

Approved for public release; distribution is unlimited.

Available from NTIS, Springfield, Virginia 22161.

12b. DISTRIBUTION CODE

13. ABSTRACT (*Maximum 200 words*)

Constitutive equations and strength criteria have been developed for ice in a multiaxial stress state. The equations developed describe the entire creep process, including primary, secondary, and tertiary creep, at both constant stresses and constant strain rates in terms of normalized (dimensionless) time $\bar{t} = t/t_m$. Secondary creep is considered an inflection point defining the time to failure (t_m). The minimum strain rate at failure is described by a modified Norton-Glen power equation, which, as well as the time to failure, includes a parabolic yield criterion. The yield criterion is selected either in the form of an extended von Mises-Drucker-Prager or an extended Mohr-Coulomb rupture model. The criteria take into account that at a certain magnitude of mean normal stresses (σ_{max}) the shear strength of ice reaches a maximum value due to local melting of ice. The model has been verified using test data on the yield of polycrystalline ice at –11.8°C and on creep of saline ice at –5°C, both under triaxial compression ($\sigma_2 = \sigma_3$).

14. SUBJECT TERMS			15. NUMBER OF PAGES
Creep	Ice	Strength	22
Failure	Model	Yield	16. PRICE CODE

17. SECURITY CLASSIFICATION OF REPORT	18. SECURITY CLASSIFICATION OF THIS PAGE	19. SECURITY CLASSIFICATION OF ABSTRACT	20. LIMITATION OF ABSTRACT
UNCLASSIFIED	UNCLASSIFIED	UNCLASSIFIED	UL